



ORIGINAL ARTICLE

LmjF.36.3850, a novel hypothetical *Leishmania major* protein, contributes to the infection

Shubhramshu Zutshi¹  | Aditya Yashwant Sarode¹ | Soumya Kanti Ghosh² | Mukesh Kumar Jha¹ | Raki Sudan¹ | Sunil Kumar¹ | Late Parag Sadhale³ | Somenath Roy⁴ | Bhaskar Saha^{1,5} 

¹National Centre for Cell Science, Pune, India

²Maulana Abul Kalam Azad University of Technology, Kolkata, India

³Indian Institute of Science, Bengaluru, India

⁴Department of Human Physiology, Vidyasagar University, Midnapore, India

⁵Trident Academy of Creative Technology, Chandrasekharpur, India

Correspondence

Bhaskar Saha, National Centre for Cell Science, Ganeshkhind, Pune 411007, India.

Email: bhaskar211964@yahoo.com

Senior author: Shubhramshu Zutshi

Funding information

The authors thank Infect-eRA and DBT for financial assistance. Fellowships to S.Z., A.S. and M.K.J. were provided by Department of Science and Technology, Department of Biotechnology, University Grants Commission, and Indian Council of Medical Research, Government of India (GoI).

Abstract

Leishmania is a protozoan parasite that resides in mammalian macrophages and inflicts the disease known as leishmaniasis. Although prevalent in 88 countries, an anti-leishmanial vaccine remains elusive. While comparing the virulent and avirulent *L. major* transcriptomes by microarray, PCR and functional analyses for identifying a novel virulence-associated gene, we identified LmjF.36.3850, a hypothetical protein significantly less expressed in the avirulent parasite and without any known function. Motif search revealed that LmjF.36.3850 protein shared phosphorylation sites and other structural features with sucrose non-fermenting protein (Snf7) that shuttles virulence factors. LmjF.36.3850 was predicted to bind diacylglycerol (DAG) with energy value similar to PKC α and PKC β , to which DAG is a cofactor. Indeed, 1-oleoyl-2-acetyl-sn-glycerol (OAG), a DAG analogue, enhanced the phosphorylation of PKC α and PKC β I. We cloned LmjF.36.3850 gene in a mammalian expression vector and primed susceptible BALB/c mice followed by challenge infection. We observed a higher parasite load, comparable antibody response and higher anti-inflammatory cytokines such as IL-4 and IL-10, while expression of major anti-leishmanial cytokine, IFN- γ , remained unchanged in LmjF.36.3850-vaccinated mice. CSA restimulated LN cells from vaccinated mice after challenge infection secreted comparable IL-4 and IL-10 but reduced IFN- γ , as compared to controls. These observations suggest a skewed Th2 response, diminished IFN- γ secreting Th1-T_{EM} cells and increased central and effector memory subtype of Th2, Th17 and Treg cells in the vaccinated mice. These data indicate that LmjF.36.3850 is a plausible virulence factor that enhances disease-promoting response, possibly by interfering with PKC activation and by eliciting disease-promoting T cells.

KEYWORDS

DNA vaccine, immunization, *Leishmania*, LmjF.36.3850, virulence

Abbreviations: CSA, crude soluble antigen; DSMD, 1,2-distearoyl-monogalactosyl-diglyceride; ESCRT, endosomal sorting complex required for transport; HP, high passage (avirulent); LN, lymph node; LP, low passage (virulent); Snf7, sucrose non-fermenting protein 7.

INTRODUCTION

Leishmania, a protozoan parasite causing a complex of diseases called Leishmaniases, interacts with multiple receptors on macrophages that play host to this pathogen. Following multiple ligand–receptor interactions [1], the parasite is internalized and transferred to endolysosomal vacuoles [2]. Once inside its host cell, the parasite expresses proteins, which interfere with host cell metabolism, signalling and antigen processing and presentation [3], resulting in immune suppression or immune deviation. Lipophosphoglycan (LPG) helps *Leishmania* achieve some of these objectives by delaying endosome maturation and acidification of phagosomes [4,5]. *Leishmania* peroxidoxins – LcPxn-1 and LcPxn-2 – reduce intracellular concentration of scavenging molecules inside macrophages [6]. Also, parasitic iron transporters, for example, LIT-1 and LIT-2, replenish intra-phagosomal Fe^{2+} , required for leishmanial metabolism and replication [7]. KMP-11 helps in amastigote replication during initial stages of infection and subsequent rise in IL-10 production but diminished NO secretion [8]. These proteins help the parasite survive within the host and are designated as virulence factors. As a working principle for formulating an anti-leishmanial vaccine, such virulence factors were proposed as potential vaccine candidates [9,10]. Lipophosphoglycan (LPG) was shown to promote the infection by heightened TGF- β release during i.m. LaAg (*L. amazonensis* antigen) vaccination, whereas intranasal vaccination with LPG reduced lesion growth, thus exerting dual role as an immune-modulatory molecule [11]. Recently, immunization with *L. mexicana* LPG has been reported to enhance PD-1 and PD-L2 expression [12]. Vaccination with KMP-11 encoding DNA reduces *L. donovani* parasite burden, while protection against *L. major* requires the presence of rIL-12 as an adjuvant [13]. These studies, although pointing towards importance of virulence factors as important vaccine candidates, indicate heterogeneity in the vaccination efficacy of *Leishmania*-expressed virulence factors.

The anti-leishmanial vaccination started with live *Leishmania* injection in Iran and Israel [14]. Due to priming-induced infection, secondary transmission and poor efficacy, live *Leishmania* was discontinued [14,15] and replaced with killed or fixed *Leishmania*. These variants of the first generation of *Leishmania* vaccine provided inconsistent and poor host protection [16]. The second generation of anti-leishmanial vaccine included multiple epitope-bearing protein antigens or the gene-modified *Leishmania* such as biopterin transporter-1 or centrin gene-deleted *Leishmania*, which allowed the parasite to ‘persist’ for a specific period of time for immune memory generation but was unable to develop chronic infection [17,18]. While pre-clinical studies showed promise, genetically modified species vaccination trial had hindrances such as virulence reversal, culture standardization and transmissibility by natural sandfly vector [19] and susceptibility of naked peptides to systemic proteases and

activation of limited repertoire of T cells posed problems for these approaches [20]. Therefore, the next strategy adopted was to identify the key virulence factors such as gp63, KMP-11, LACK, HASPB1 and many others [10,18]. Although many of these candidates elicited host-protective immune responses characterized by increased IFN- γ -secreting Th1 cells or reduced IL-4-secreting Th2 or suppressive Treg cells, these candidates showed poor efficacy in human trials [21,22].

Addressing these problems for designing a potential anti-leishmanial vaccine, we first compared the transcriptomes from two virulent and corresponding avirulent strains of *L. major* through several steps. Finally, we identified LmjF.36.3850, a hypothetical protein, to which no function is assigned till date. Its expression was significantly downregulated in the avirulent *L. major* parasite, implying this as a potential virulence factor and therefore a plausible DNA vaccine candidate. This hypothetical protein share motifs with Snf7 family, key virulence factors in *Cryptococcus neoformans* necessary for transporting virulence factors to its surface. LmjF.36.3850 and Snf7 share homology in amino acid sequences and PKC phosphorylation sites. 1,2-Distearoyl-monogalactosyl-diglyceride (DSMD), a structural homologue of DAG, an activator of PKC α and PKC β , is predicted to be the most favourable ligand for LmjF.36.3850, implying competitive inhibition of the DAG-dependent PKC isoforms, implicated in the skewing of signalling. Supplementing *L. major*-infected macrophages (IM) with OAG resulted in increased phosphorylation of PKC α and PKC β 1 and subsequent increase in IL-12 and decrease in IL-10 secretion. Further, we cloned LmjF_36_3850 gene in a mammalian expression vector and immunized *Leishmania*-susceptible BALB/c mice with this gene. The vaccination enhanced the disease instead of providing any host protection. However, despite the increased disease-promoting functions in the LmjF.36.3850-immunized mice, the parasite load did not significantly increase suggesting dissociation of the vaccine-elicited immune response from the outcome of the challenge infection.

MATERIALS AND METHODS

Mice, macrophages, in vitro parasite infection and stimulation

Female BALB/c mice from the Jackson Laboratories were bred at the Institute's animal facility. 6- to 8-week-old mice were used following Institutional Animal Care and Use Committee approved protocols. Thioglycolate (DIFCO; i.p., 3%, 2 ml)-elicited macrophages were cultured in GIBCO[®] FBS (Thermo Fisher Scientific)-supplemented RPMI-1640, infected with in vitro-cultured [23] *L. major* strain (MHOM/Su73/5ASKH; LP or HP) promastigotes at a 1:10 macrophage:parasite ratio [24]. BD Pharmingen[™] Recombinant IFN- γ and BD Pharmingen[™] Purified NA/

LE Rat Anti-mouse CD40 antibodies (clone 3/23; BD Biosciences) were used for macrophage stimulation. Macrophages were kept for 8 and 64 h post-infection before rIFN- γ and anti-CD40 stimulation, respectively.

RNA isolation and quantitative real-time PCR

cDNA was prepared from RNA (macrophage, LN cells) isolated using TRI reagent (Sigma-Aldrich) [24,25]. qPCR was performed using SYBR premix containing Tli RNaseH (Takara Bio USA) and gene-specific primers (0.2 μ mol) (IDT Inc.) on a StepOnePlus (Applied Biosystems Inc.) under following conditions: 95°C (30 s), 45 cycles of 95°C (5 s) and 60°C (34 s). Reactions were performed in duplicates, and mRNA levels of genes were normalized against β -tubulin of *L. major* while analysing leishmanial genes or GAPDH of mice for analysing mice-specific genes [26]. The gene-specific primers used for amplification are shown in Table 1.

Conserved motif prediction

We used four platforms for motif search – NCBI-CDD (motif search) [27], EMBL_EBI-supported Pfam [28] (motif search), InterPro [29] and PROSITE [30] (MyHits, SIB) – using LmjF.36.3850 protein sequence as input. Clustal Omega [31] was used for multiple protein sequence alignments.

Protein sequence

NCBI ref no. of PKC isoforms and UniProt ref. no. of Snf7 are as follows – PKC alpha: NP_035231.2, PKC beta iso1: NP_0.32881.1, PKC beta iso2: NP_00.1303601.1, PKC epsilon: NP_035234.1, PKC lambda: BAA32499.1, PKC delta iso1: NP_001297611.1, PKC delta iso2: NP_035233.1, LmjF_36_3850: XP_001686968.1, and SNF7 sequence: P39929.

TABLE 1 Sequence of primers used for real-time PCR

Gene	Primer Sequence: Forward	Primer Sequence: Reverse
Coproporphyrinogen iii oxidase	FP: 5'-CCTCTTCTTCGACGACCTTAAC-3'	RP: 5'-TGGGATGTACGCATCAATGTAG-3'
Methionine aminopeptidase 2	FP: 5'-CAAGGTGCACCAGGTAAAGA-3'	RP: 5'-TTGCCGCTATGGATGATGTAG-3'
Transaldolase	FP: 5'-GGTGTGTCTCCGTCCTAAG-3'	RP: 5'-CAGCTCCAAGATCTCCTCAAC-3'
Ubiquitin-conjugating enzyme	FP: 5'-CCGCCAGACATTCTCTCTTTA-3'	RP: 5'-CTTGTGGTAGCTGCTGATAGTC-3'
p-nitrophenylphosphatase	FP: 5'-CCTTGACATCCAGGAGAAGTT-3'	RP: 5'-GACGGACTGCACCTCATTAT-3'
GP63, leishmanolysin	FP: 5'-TACGAGGAAAGCCGCATAAC-3'	RP: 5'-ATCCTCCATCTCCAGATACTCC-3'
NAD+synthase	FP: 5'-CTTCCCGTACGACTTTGTAGAG-3'	RP: 5'-GTTTCGGGCCTCATCACATA-3'
Adenylate kinase	FP: 5'-AGGAAGCGTCAGGATGAATAC-3'	RP: 5'-CGAGCAACTTCGGCAAATAC-3'
Adenine phosphoribosyltransferase	FP: 5'-AGATCCACTCGACAGGTCATA-3'	RP: 5'-GAGGACCCGTGTAGTTCCTTTG-3'
DNA polymerase epsilon subunit B	FP: 5'-GTGCGGGATGACGAAGTATT-3'	RP: 5'-CCACAGTCAGGAACCCATTT-3'
Hypothetical protein LmjF.36.3850	FP: 5'-GGATGAGCTGAAGCGTTCTAA-3'	RP: 5'-CTTGTCCATCTCCTCCATCAAG-3'
Iron superoxide dismutase	FP: 5'-TCGGCAGCTTCTCGAATTT-3'	RP: 5'-CCACTCGACTTGTCTTTCAC-3'
Sphingolipid δ 4 desaturase	FP: 5'-CTAATGTGGAATGTCGGCTATCA-3'	RP: 5'-CGTAGAACTCCGGTGAATAG-3'
Hypothetical protein LinJ07.0020	FP: 5'-TGATAGCTCCGAGGAAGATGAG-3'	RP: 5'-CACTGGATCCCAACCACTTTAC-3'
2-Oxoisovalerate dehydrogenase α subunit	FP: 5'-CAATACAGAGAGGGCGGTATTTC-3'	RP: 5'-CTTGCTGCCGTAGTGGATAG-3'
Phosphatidic acid phosphatase	FP: 5'-GCATCTTACGGGTCTTCTT-3'	RP: 5'-GTCGAAGTAGTGACGGTTGTC-3'
Thiol-dependent reductase 1	FP: 5'-CGATCTCTTCGCCACTTT-3'	RP: 5'-CGGATGTGCTCCTTGTACTC-3'
Aldehyde dehydrogenase, mito precursor	FP: 5'-GTCTGGTAAGACATTCGAGGTT-3'	RP: 5'-GCATTCACAGCAAGGTTTAC-3'
Pyruvate/indole-pyruvate carboxylase	FP: 5'-CACAAGATCGACCCTCTCAA-3'	RP: 5'-ACTTCTTCGACCGCCTTTAC-3'
HGPRT	FP: 5'-CCGTGGAGAATCGCCATATT-3'	RP: 5'-GAGCATGAACCGCATCAGATA-3'
Hypothetical protein LmjF.36.4610	FP: 5'-GCGATGAACGAGGTAGAGAAG-3'	RP: 5'-ACGAGAACAGCCATGCATAA-3'
Hypothetical protein LmjF.33.2620	FP: 5'-CCGTGCGTTTAAGCACTTTC-3'	RP: 5'-CCCAAACACCAAGAACAACAAC-3'
Hypothetical protein LinJ25.2100	FP: 5'-GTCATTCTGGCCTGTTTCT-3'	RP: 5'-CCGATGCTGATGAAGGTGAA-3'
ARP2/3 complex subunit	FP: 5'-TATTGAGGCATCGTGTGACAG-3'	RP: 5'-GAGCAGAAGAACGCCATGTA-3'
Hypothetical protein LinJ35.2730	FP: 5'-TGGACGTGAAGGAGCTTATTG-3'	RP: 5'-CAGCACAGAGCGAATCTCTT-3'
β -tubulin	FP: 5'-AGCAGTTCACGGGTATGTTTC-3'	RP: 5'-GAGACGAGGTCGTTTCATGTT-3'

Secondary structure prediction

Structure prediction was conducted using I-Tasser server-based threading, assembling and refinement techniques. The prediction is accomplished in four stages, Stage 1 – threading: template sequences from BLAST are used for structure prediction using PSIPRED. The sequences and the respective structured queries are threaded using LOMETS, which uses seven programs (FUGUE, HHsearch, MUSTER, PROSPECT, PPA, SP3 and SPARS) to individually rank templates based on sequence and structure ranking, and then, results from each are judged based on statistical significance. Stage 2 – structural assembly: fragments that continuously align to sequence of interest are excised from the template and assembled. The structural conformations are built from the aligned fragments using ab initio modelling replica-exchange Monte Carlo simulation techniques (knowledge-based simulation), and the confirmations with lower free energy are sorted by SPIKER. For the non-aligned parts, the deviation is restricted to 0.84 Å. Stage 3 – model selection and refinement: the fragment assembly models are simulated again to remove steric hindrance and optimize the hydrogen bonding networks. The lowest energy models are screened using REMO program. Stage 4 – structure-based functional annotation: for prediction accuracy, confidence score (C-score) was generated using the equation:

$$C - \text{score} = \ln [M/M_{\text{tot}} \times 1/\text{RMSD} \times 1/7 \sum_{i=1}^7 Z_{(i)}/Z_{0(i)}]$$

M : structure decoys in a cluster; M_{tot} : total numbers of decoy predicted; RMSD: average RMSD of decoys against the cluster centroids; $Z_{(i)}$: best template predicted by i th thread from the seven LOMETS; $Z_{0(i)}$: Z-score cut-off to differentiate between good and bad templates.

The series of few highest C-score templates used to construct LmjF.36.3850 are PDB.id C6ZH3A, C5FD7A, C5J45A, C5VO5A, C2GD5B, C3FRVA, C3FRTB, C4ABMC, C2LUHB, etc. The sequence of each protein is submitted to server without any specific parameter defined, and the structure generated is obtained with the set parameters of the I-Tasser Server [32]. Homology modelling-generated structure of Snf7 is obtained using PDB Id: 5T8L.1.A (vacuolar-sorting protein SNF7) with 100% sequence identity.

Ligand prediction and molecular docking

Ligand prediction is performed using ProBiS-ligands online server [33], where prediction binding site distance was capped within 3 Å. ProBiS algorithm superimposes protein surfaces, protein surface motifs and protein binding sites, enabling pairwise alignment and search for binding sites in database. The algorithm also identifies binding sites from proteins having different fold without information of locations.

SwissDock is an online server using docking software EADock DSS, which allows docking small molecules onto a receptor by generating binding modes in all target cavities; we further checked for favourability using CHARMM force field in an estimated grid. The predicted docking complexes are evaluated with FACTS and presented.

Transfection of RAW264.7 macrophages

RAW264.7 are seeded in a 6-well tissue culture dish and transfected at 70%–80% confluency with either pcDNA6/HisA- or LmjF_36_3850-cloned pcDNA6/HisA by Lipofectamine™ 3000 reagent (Invitrogen) as per the manufacturer's instructions. Briefly, 3 µg DNA was diluted in optiMEM along with 6 µl P3000 reagent and 3.75 µl Lipofectamine 3000 reagent was diluted in optiMEM in another tube. Diluted DNA tube was added to diluted Lipofectamine tube (1:1 ratio), and complex was added to cells dropwise. After 8-h transfection, fresh media were added to cells without replacing optiMEM. Transfected cells were kept for 48 h post-transfection and processed for lysis and Western blotting analysis.

OAG supplementation of macrophages

Macrophages were infected with stationary phase *L. major* promastigotes at a macrophage:parasite ratio of 1:10 for 6 h as described previously in this section. 1-Oleoyl-2-acetyl-sn-glycerol (OAG; MilliporeSigma) was supplemented to culture medium at the PKC-activating dose determined by dose and time kinetics. For western transfer, media were immediately removed afterwards; cells were washed with ice-cold PBS and lysed in NP-40 buffer containing protease inhibitor cocktail (Roche Holding AG) and phosphatase inhibitor (sodium orthovanadate; MilliporeSigma).

Western blotting

Protein lysate prepared in NP-40-containing buffer was centrifuged at 20 000 g for 30 min, and the supernatant was obtained. Protein content was quantified by Pierce™ BCA protein assay kit. Equal amount of lysate for each sample was run on denaturing SDS-PAGE. Resolved proteins were transferred onto PVDF membrane and blocked in 5% non-fat dry milk prepared in Tris-buffered saline containing 0.1% Tween-20 (TBS-T). Membrane was incubated overnight with primary antibody (1:1000) at 4°C, washed thrice with TBS-T, incubated with HRP-conjugated secondary antibody (1:3500 for anti-rabbit and anti-mouse IgG and 1:2000 for anti-goat IgG) and washed thrice with TBS-T. Membrane was probed and visualized with ClarityMax™ Western ECL Substrate

(Bio-Rad Laboratories). Antibodies used for immunoblotting were purchased from Cell Signaling Technology– phospho-PKC α (9375); Santa Cruz Biotechnology– PKC α (sc-208), p-PKC β I (sc-101776), PKC β I (sc-209), Actin (sc-1616) and donkey anti-goat IgG HRP (sc-2020); Bio-Rad Laboratories– goat anti-rabbit IgG HRP conjugate (1706515) and goat anti-mouse IgG HRP conjugate (1706516).

Molecular cloning of LmjF_36_3850 in pcDNA6/HisA vector

LmjF_36_3850 was amplified in a thermal cycler (Eppendorf Inc.) using Phusion[®] High-Fidelity Taq Polymerase (New England Biolabs) using primers: sense, 5'-TATCGCGGATCCTGATGTTCAATCGTCTC-3'; antisense, 5'-TATCTGCTCTAGAGTTACGCAAGCTCCGC-3' (IDT Inc.). Amplified PCR product was purified by GenElute[®] PCR purification kit (Sigma-Aldrich). pcDNA6/HisA and purified PCR product were subsequently digested by BamHI and XbaI (New England Biolabs) at 37°C for 4 h, and gel-eluted using GenElute[®] Gel Extraction Kit (Sigma-Aldrich). A ligation reaction was set up according to protocol supplied along with T4 DNA Ligase (New England Biolabs). Cloning confirmation was done by digesting plasmids with same set of enzymes and Sanger sequencing.

Subcellular fractionation

Macrophages in a 100-mm culture dish were infected with stationary phase *L. major* promastigotes as described in Mice, macrophages, in vitro parasite infection and stimulation. Uninfected and infected cells from two 100-mm dishes were pooled together. Cells were homogenized in 700 μ l HES buffer (20 mM HEPES; pH 7.6, 1 mM EDTA, 255 mM sucrose) containing PI using a 26-gauge needle. Cytoplasmic fraction was separated [34], quantified by BCA assay and used for immunoblotting.

In vitro transfection in HEK293 T cells

Cloned vector was transfected into HEK293T cells by Effectene[®] transfection reagent (Qiagen Inc.) as per the manufacturer's instructions, and transcript level LmjF_36_3850 expression was determined after 48 h in transfected and non-transfected cells by semi-quantitative PCR at 95°C for 3 min, 36 cycles of 94°C for 1 min, 57°C for 1 min and 72°C for 1 min followed by 72°C for 10 min in a thermal cycler. Primers used were as follows: LmjF_36_3850 sense, 5'-ATGTTCAATCGTCTCTTTGGCAG-3'; antisense, 5'-TTACGCAAGCTCCGCCTC-3' (IDT Inc.).

Immunization of mice, in vivo expression of LmjF.36.3850 and *L. major* challenge

For immunization, endotoxin-free DNA was prepared by caesium chloride (Sigma-Aldrich) density gradient centrifugation at 1 80 000 *g* for 14 h at 25°C in Optima MAX[™] ultracentrifuge (Beckman Coulter Inc). Hundred microgram of either cloned or control DNA in 100 μ l HBSS (pH 7.4) was injected (i.m) three times at 15-day intervals. 100 μ g of cloned DNA was injected (i.m.) in BALB/c mice, and LmjF_36_3850 was assessed 4 days post-injection in isolated tissue by RT-PCR. Four weeks after the last immunization, 2×10^6 stationary phase *L. major* promastigotes were injected in the left hind footpad. Footpad swelling was weekly measured. On the 5th week, parasite load in draining LN was assessed [24].

Serum antibody titre and anti-LmjF.36.3850 IgG determination

Sera were prepared from naïve, immunized but either infected or uninfected mice for detection of *Leishmania*-specific IgG antibodies by indirect ELISA using biotin-labelled anti-mouse IgG2a and IgG1 (BD Biosciences) and developing the reaction by BD OptEIA[™] TMB substrate [35]. Virulent *Leishmania* culture was resuspended in 20 mM Tris (pH 7.5), 150 mM NaCl, 1 mM each of EDTA and EGTA, 10% glycerol and 1% NP-40, diluted in sample buffer and probed with sera from empty or cloned vector primed mice in varying dilutions as indicated and detected with 1:5000 diluted HRP anti-mouse IgG (Bio-Rad Laboratories).

Cytokine (sandwich) ELISA

Culture supernatants from either unstimulated/CSA-stimulated lymphocytes, macrophage T-cell co-culture or macrophage culture were collected and spun at 300 *g* for 5 min. IL-10, IL-12, IL-4 and IFN- γ levels were determined as described previously [36].

Macrophage T-cell co-culture

5×10^4 thioglycollate-elicited peritoneal macrophages were in vitro-infected with *L. major* as previously described in material and methods. After 36 h of infection, lymphocytes from different groups were added to the culture supernatant and incubated for 72 h. Culture supernatant was collected and assessed for IL-12 and IL-10 production by ELISA.

Multi-chromatic Flow cytometry

LN cells from each group were stimulated for proliferation [37]. Following blockade with FBS, cells were incubated with cell membrane-specific antibodies in PBS (pH 7.4) containing 10 mM HEPES and 3% FBS for 1 h. Cells were permeabilized with 150 μ l of BD Cytotfix/Cytoperm™ (BD Biosciences) for 20 min and washed twice with PBS (pH 7.4) containing 10 mM HEPES, 3% FBS and 0.1% saponin. Cells were incubated with intracellular molecule-specific antibodies for 75 min. Cells were acquired, data recorded on

BD Canto-II and analysed with FACSDiva 6.0 software (BD Biosciences).

Antibodies used for flow cytometry were procured from: (a) BD Biosciences – FITC anti-mouse CD3 (555274), PB anti-mouse CD4 (558107), PerCP-Cy5.5 anti-mouse CD44 (560570), APCy7 anti-mouse CD62L (560514), PECy7 anti-mouse CD25 (552880), PE anti-mouse IFN- γ (554412), PE anti-mouse IL-4 (18195A), PE anti-mouse IL-10 (554467), APC anti-mouse IL-12 (554480), APC anti-mouse FOXP3 (563486) and PECy7 anti-mouse CD11b (552850); (b) Biolegend – APC anti-mouse T-bet (644804), APC anti-mouse

TABLE 2 qPCR validation of genes selected from microarray analysis^a

No.	Gene name	Gene description	Promastigote	Amastigote
1	LinJ06.1320	Coproporphyrinogen iii oxidase	UP	UP
2	LinJ32.2230	Hypoxanthine-guanine phosphoribosyltransferase	UP	UP
3	LinJ05.0940	Methionine aminopeptidase 2	UP	UP
4	LinJ31.3030	Iron superoxide dismutase	DOWN (ND/HP)	DOWN (ND/HP)
5	LinJ34.2770	Pyruvate/indole-pyruvate carboxylase	UP	UP
6	LinJ10.0780	GP63, leishmanolysin	UP	UP (ND/LP)
7	LinJ12.0120	p-nitrophenylphosphatase	---	UP (ND/LP)
8	LmjF26.1700	Fatty acid desaturase; sphingolipid δ 4 desaturase	UP	UP (ND/LP)
9	LmjF35.1790	DNA polymerase epsilon subunit B	UP	UP
10	LmjF25.1120	Aldehyde dehydrogenase, Mitochondrial precursor	DOWN	UP ((ND/LP)
11	LmjF18.0440	Phosphatidic acid phosphatase	DOWN	DOWN
12	LmjF25.2370	Adenylate kinase	DOWN	Not detected
13	LmjF32.1670	NAD ⁺ synthase	DOWN	DOWN (ND)
14	LmjF36.3850	Hypothetical protein	DOWN	DOWN
15	LinJ07.0020	Hypothetical protein	DOWN	UP (ND/LP)
16	LmjF26.0140	Adenine phosphoribosyltransferase	DOWN	DOWN
17	LmjF33.2620	Hypothetical protein	–	DOWN (ND/HP)
18	LinJ21.1970	Ubiquitin-conjugating enzyme	DOWN	DOWN
19	LmjF17.0190	Receptor type adenylate cyclase	DOWN	DOWN
20	LmjF36.6390	Methylene tetrahydrofolate reductase	DOWN	UP (ND/LP)
21	LmjF33.0240	Thiol-dependent reductase 1	DOWN	DOWN
22	LinJ21.1100	2-Oxoisovalerate dehydrogenase α subunit	UP	Not detected
23	LinJ16.0790	Transaldolase	DOWN	UP
24	LmjF03.0980	eIF-2 alpha subunit	DOWN	UP
25	LmjF22.0310	Carnitine palmitoyl transferase like protein	DOWN	UP
26	LmjF32.2640	Cystathionine beta lyase	DOWN	UP
27	LmjF36.0890	Eukaryotic translation initiation factor (eIF-6)	UP	No change
28	LmjF02.0600	ARP 2/3 complex subunit	DOWN	Not detected
29	LmjF36.4610	Hypothetical protein	DOWN	Not detected
30	LinJ25.2100	Hypothetical protein	DOWN	UP
31	LinJ35.2730	Hypothetical protein	DOWN	UP

^aSelected genes from microarray analysis were subsequently analysed by qPCR for their relative expression in virulent and avirulent forms during promastigote and amastigote life stages. Genes were selected from microarray results of 5ASKH, LV39, Ag83 and LV9 strains, and representative qPCR results for 5ASKH are shown here. 'UP' and 'DOWN' indicate the upregulated and downregulated expression in HP as compared to LP strain of 5ASKH for respective genes. ND/'strain type' indicate undetectable gene expression in respective strain of 5ASKH.

IL-17a (506916) and APCCy7 anti-mouse F4/80 (123118); and (c) eBioscience, Inc. – APC anti-mouse GATA-3 (50-9966-42) and PE anti-mouse ROR γ t (12-6981-82).

Statistical analysis

In vitro cultures were done in duplicates, and five mice were used per group for in vivo experiments. Results shown are indicative of two independent vaccination experiments. Statistical analysis was performed by SigmaStat 3.5 (Systat Software, Inc.). Data were computed for significance between groups using one-way ANOVA employing the Student–Newman–Keuls test, and $P \leq 0.05$ was considered significant.

RESULTS

We performed *Leishmania* whole-genome microarray analysis (Tables S1,S2) to identify the genes that showed different FLAG values (A or P) in either virulent (LP) or avirulent (HP) form of *L. major* strains (5ASKH and LV39). We first compared the genes showing a fold change >2 (either upregulated or downregulated). We filtered common genes occurring

among the compared strains and selected 31 genes for validation by qPCR (Table 2). After qPCR analysis, we found that 21 out of those 31 genes showed significantly altered expression between the virulent (LP) and avirulent (HP) *L. major* strains. Finally, after sequence alignment ($<50\%$ match with *Mus musculus* and *Homo sapiens* in blastp) and contiguous sequence match (<11 identical contiguous amino acids), we finally selected 12 genes for further studies (Table 3). The aforementioned strategy for virulence factors selection is shown in Figure 1a. We validated the expression of these 12 genes by qPCR after in vitro infection of primary macrophages with virulent or avirulent 5ASKH strains. We tested the importance of these genes in host response by treating these macrophages with IFN- γ or anti-CD40 antibody that acts as a CD40 agonist.

Leishmanial genes show differences in expression between virulent and avirulent amastigotes

NAD $^{+}$ synthase, LmjF.36.3850, phosphatidic acid phosphatase (PAP), thiol-dependent reductase-1 (TDR), LmjF_33_2620 and ARP 2/3 kinase were significantly downregulated inside

TABLE 3 In silico analysis of Leishmanial genes selected from qPCR^a

S. No.	Protein	% identity (<i>Mus musculus</i>)	% identity (<i>Homo sapiens</i>)	Contiguous stretch of >11 amino acids
1.	DNA polymerase ϵ subunit B	26	25	No
2.	Pyruvate Carboxylase	29	30	No
3.	p-nitrophenylphosphatase	36	35	No
4.	Aldehyde dehydrogenase	46	48	Yes
5.	Coproporphyrinogen III oxidase	45	46	Yes
6.	Fatty acid desaturase	44	46	Yes
7.	gp63 Leishmanolysin	27	24	No
8.	Methionine aminopeptidase	60	57	Yes
9.	NAD $^{+}$ synthase	26	22	No
10.	Thiol-dependent reductase-1	24	33	No
11.	2-Oxoisovalerate dehydrogenase	46	46	Yes
12.	Adenine phosphoribosyltransferase	47	42	Yes
13.	Adenylate kinase	37	46	No
14.	ARP 2/3 kinase	43	49	No
15.	Iron superoxide dismutase	38	41	Yes
16.	Phosphatidic acid phosphatase	40	36	No
17.	Ubiquitin-conjugating enzyme E2	71	70	Yes
18.	HGPRT	None	None	No
19.	LmjF_36_4610	39	42	No
20.	LmjF.36.3850	34	44	No
21.	LmjF_33_2620	33	32	No

^aProtein sequences of listed Leishmanial genes were subjected to blastp with mouse and human proteome for sequence alignment and similar stretch of amino acids.

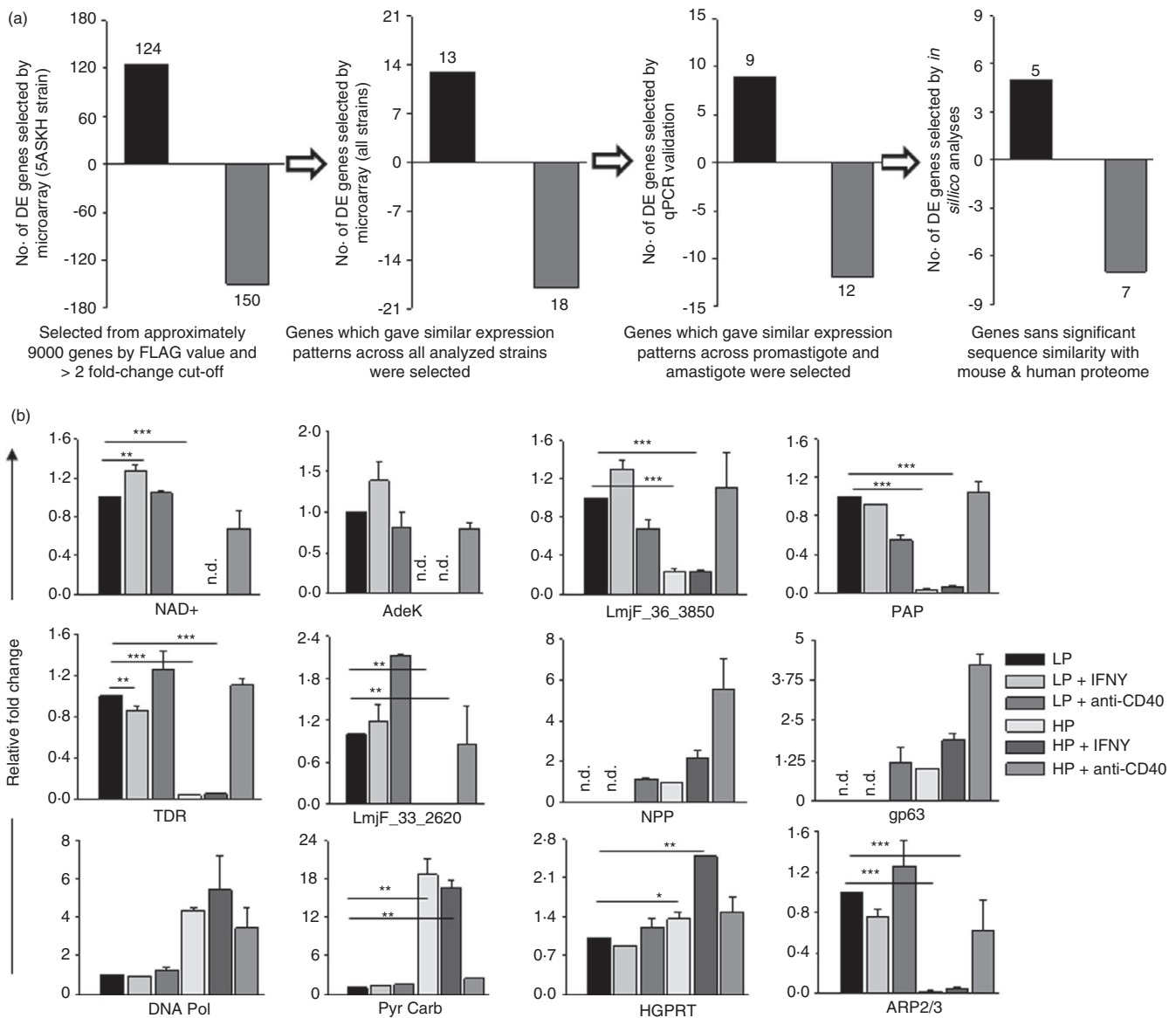


FIGURE 1 Transcriptomic analysis of *Leishmania* for identification of potential virulence factors (a) Schematic representation of methodology for selecting the probable virulence factors of *Leishmania*. Numbers in bracket indicate the number of genes fulfilling the mentioned criteria at each step described elsewhere. Vertical bars on positive y-axis and negative y-axis represent the number of upregulated and downregulated genes in HP as compared to LP strain selected in successive steps by microarray, qPCR or in silico method as indicated. (b) Differential expression of Leishmanial genes in virulent and avirulent *L. major* strain-infected primary macrophages. RNA was isolated from the *L. major*-infected macrophages (LP and HP) cultured in the presence or absence of IFN- γ (20 ng/ml, 8 h) and anti-CD40 NA/LE (3 μ g/ml, 8 h). Relative mRNA expression of indicated genes was assessed by quantitative PCR using β -tubulin as housekeeping gene control. n.d. represents the samples where no quantifiable amplification was obtained during PCR run. The data shown here are representative of two independent experiments, and error bars indicate mean \pm SEM (* indicates $p \leq 0.05$, ** indicates $p \leq 0.01$, *** indicates $p \leq 0.001$).

avirulent *L. major*-IM, while pyruvate carboxylase (Pyr Carb) and hypoxanthine-guanine phosphoribosyltransferase (HGPRT) were significantly upregulated in avirulent *L. major*-IM. No amplification of adenylate kinase was observed in HP-IM, and similar results were obtained with n-nitrophenyl phosphatase (NPP) and gp63 in LP-IM, while NAD⁺-synthase remained undetected when HP-IM were treated with IFN- γ . Failure to amplify such genes implies that transcript copy number remained lower than the detection level post-amplification. LmjF.36.3850 expression was higher in virulent *L. major*-IM and was further augmented

by IFN- γ treatment implying LmjF.36.3850 as a virulence or virulence-associated factor (Figure 1b).

LmjF.36.3850 share motif, sequence homology and phosphorylation site residues with Snf7

Because LmjF.36.3850 is a hypothetical protein with no assigned function [38], we examined its plausible association with *Leishmania* virulence by using four

platforms – NCBI-CDD, Pfam, InterPro and PROSITE – for motif search. Common to all the motifs that came out of searches using these platforms was a motif (Figure 2a) shared by LmjF.36.3850 and Snf7 protein family. Snf7 is a part of Endosomal Sorting Complex Required for Transport (ESCRT)-III complex, which is assigned for protein sorting and traffic from endosomes to the vacuole [39]. By its indispensable role in the secretion of virulence factors, Snf7 mediates the expression of virulence of the eukaryotic pathogen *C. neoformans* [40]. Sharing of the structural motif and sequence homology by LmjF.36.3850 and Snf7 implies a possible role for LmjF.36.3850 in the execution of *L. major* virulence. Similar PKC phosphorylation sites, conforming to helical structure in both LmjF.36.3850 and Snf, imply a functional similarity (Figures 2b,c and 3a).

LmjF.36.3850 favourably binds to DAG forming a stable complex

ProBiS generated ligand prediction for LmjF.36.3850-identified DSMD, a small molecule structurally similar to DAG, as the most favourable ligand (Figure 3b–d). As activation of PKC α and PKC β isoforms are DAG-dependent, we performed docking simulations. We observed that DAG interacted with Asp213, Asp424 and Arg307 of LmjF.36.3850, PKC α and PKC β , respectively, via its glycerol moiety. Although the residues are polar with a

lower hydrophobicity value, these regions are located in internal regions of these proteins, predicting a stable ligand–receptor complex (Figure 4a). This is reaffirmed by the comparable Gibbs free energy values of the docked complexes, where the values of LmjF.36.3850-DAG complex were comparable to those of the PKC α -DAG and PKC β -DAG complex (Figure 4b). This led us to hypothesize that scavenging of DAG by competitive binding of LmjF.36.3850 may be in part responsible for decrease in DAG-dependent PKC phosphorylation observed during *L. major* infection.

LmjF.36.3850 overexpression reduces PKC phosphorylation, and OAG supplementation increases the DAG-dependent PKC phosphorylation and inflammatory response

To strengthen a probable relationship between LmjF.36.3850 and PKC α and PKC β phosphorylation, we overexpressed LmjF.36.3850 in RAW264.7 by chemical-based transfection. Expressing LmjF.36.3850 in macrophages leads to a decrease in phosphorylated forms of DAG-dependent anti-leishmanial PKCs, viz. PKC α and PKC β I (Figure 5a). We confirmed successful expression of LmjF.36.3850 post-transfection by probing its presence in cell lysate with blood sera obtained from LmjF.36.3850-primed mice. This suggests LmjF.36.3850's involvement in decreasing the pro-inflammatory PKC isoform activation. As we previously observed favourable

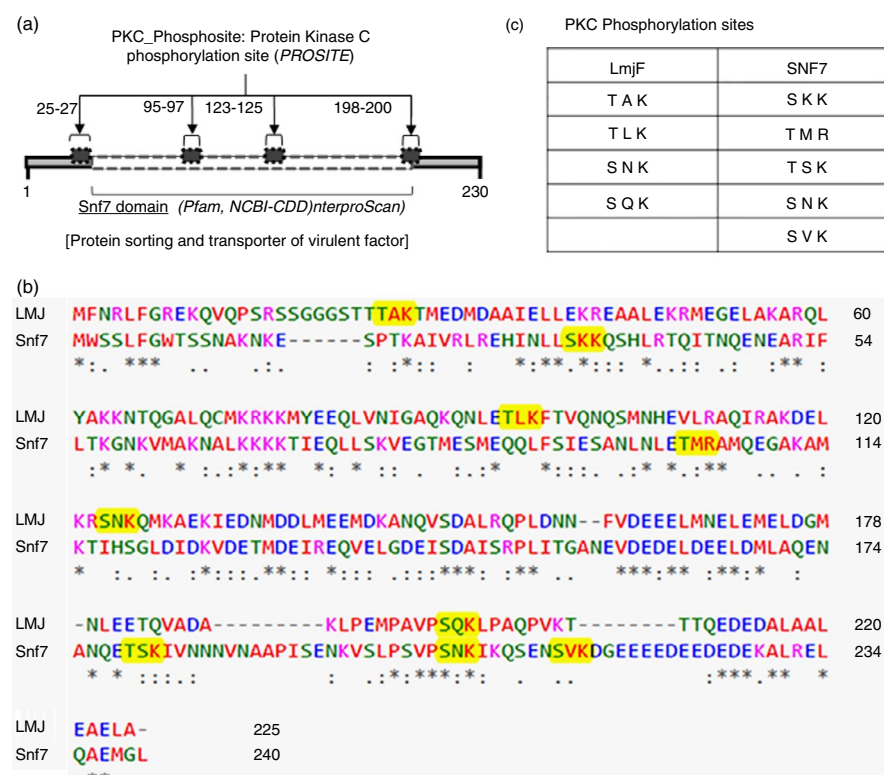


FIGURE 2 Functional annotation of LmjF.36.3850 (abbreviated LMJ and LmjF in figure) from its amino acid sequence (a) In silico-conserved domain and motif prediction was done using multiple platforms, for example MOTIF search (output from Pfam), NCBI-CDD, MyHits by SIB (output from Pfam, PROSITE) and InterProScan. We searched for multiple motifs for the entire length. Default cut-offs of each platform used to obtain results, even the parameters for each motif prediction platform are their default forms (b) Sequence alignment (Clustal Omega) and (c) PKC phosphorylation sites of LmjF.36.3850 and Snf7

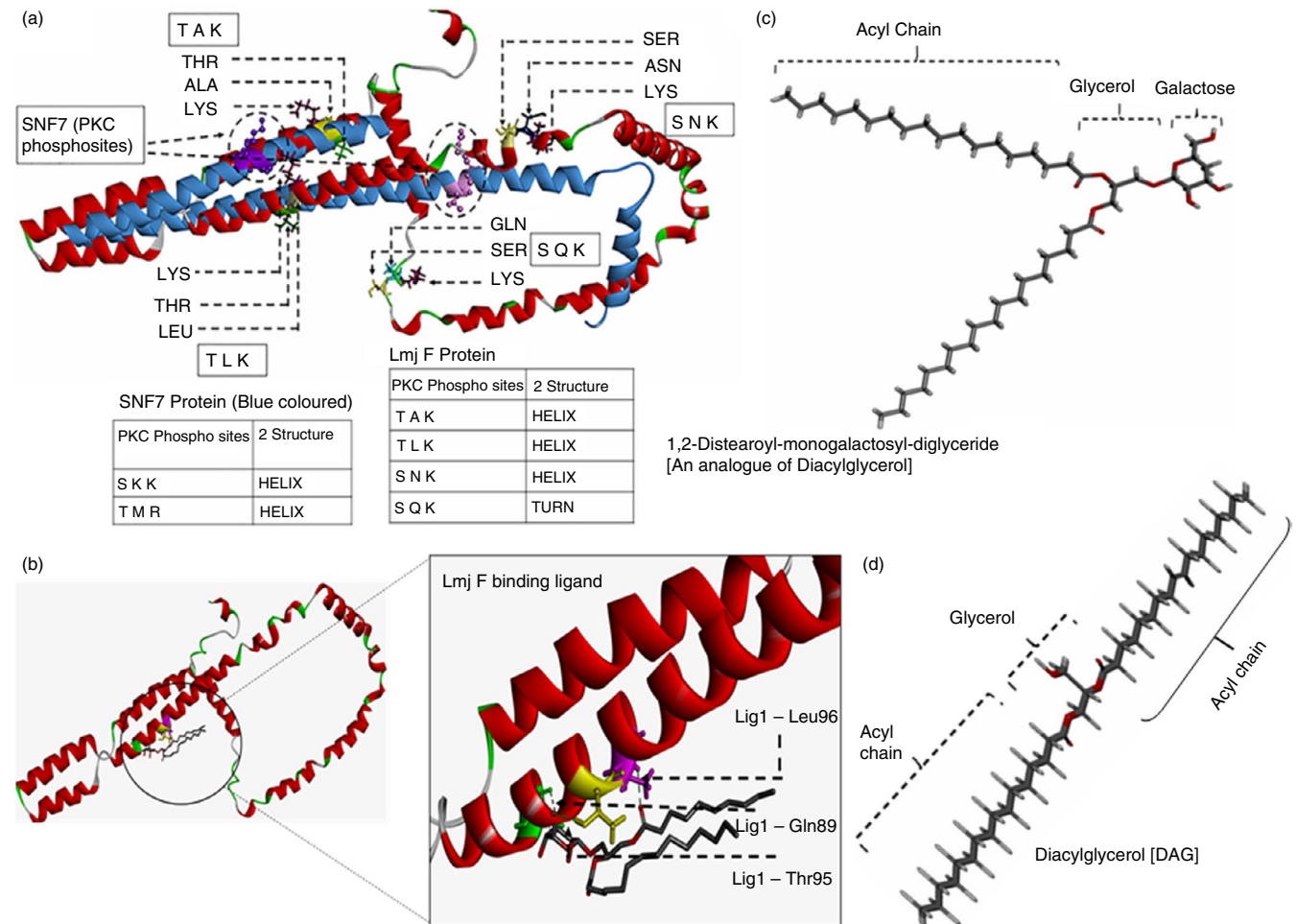


FIGURE 3 Secondary structure and ligand prediction for LmjF.36.3850. (a) Predicted secondary structure and confirmation of phosphorylation sites of LmjF.36.3850 (abbreviated LmjF in figure). LmjF.36.3850 (red) exhibits conformational similarity with Snf7 (Blue). I-TASSER-generated 3D structures are superposed, and the PKC phosphorylation sites are marked for both proteins. (b) Docking simulation of LmjF.36.3850 with its predicted favourable ligand, 1,2-distearoyl-monogalactosyl-diglyceride (DSMD) (c) 3D structure of DSMD and (d) DAG (diacylglycerol)

binding parameters in docked LmjF.36.3850-DAG complexes and favourable interactions between docked structures of LmjF.36.3850 and DAG as shown in the previous section, we checked whether this interaction has any role to play in LmjF.36.3850-induced decrease in PKC phosphorylation.

Dose and time kinetics were performed to identify the PKC-activating dose of cell-permeable DAG analogue (OAG). PKC α phosphorylation increased 5 min post-OAG addition as seen in other studies [41] at a dose of 100 μ M and was selected for further studies (Figure 5b). Next, OAG supplementation to *L. major*-IM was able to increase the phosphorylation of PKC α and PKC β 1 (Figure 5c). Furthermore, this increase in PKC α and PKC β 1 activation is linked to the increase in inflammatory response, whereby an increase in IL-12 and reduction in IL-10 secreting macrophages were seen after OAG supplementation (Figure 5d,e). OAG may thus rescue the *Leishmania*-induced interference in DAG-dependent PKC phosphorylation and therefore increase inflammatory response. Overall, these observations point

to the fact that LmjF.36.3850-induced decrease in PKC α and PKC β activation is reversed by supplying OAG to *L. major*-IM.

LmjF.36.3850 vaccination elicits anti-LmjF.36.3850 antibodies and a mixed Th response

We PCR-cloned LmjF.36.3850 in an eukaryotic expression vector pcDNA6/HisA (Figure 6a) and tested its immunogenicity and efficacy as a vaccine candidate. After in vitro and in vivo confirmation of LmjF.36.3850 expression (Figure 6b), specificity of LmjF.36.3850 vaccination-induced immune response was determined by Western blotting. Sera from vaccinated BALB/c mice detected LmjF.36.3850 in the virulent *Leishmania* lysate (Figure 6c) suggesting the immunogenicity of LmjF.36.3850.

LmjF.36.3850 was detected from IM lysate confirming that the protein is indeed expressed during intracellular

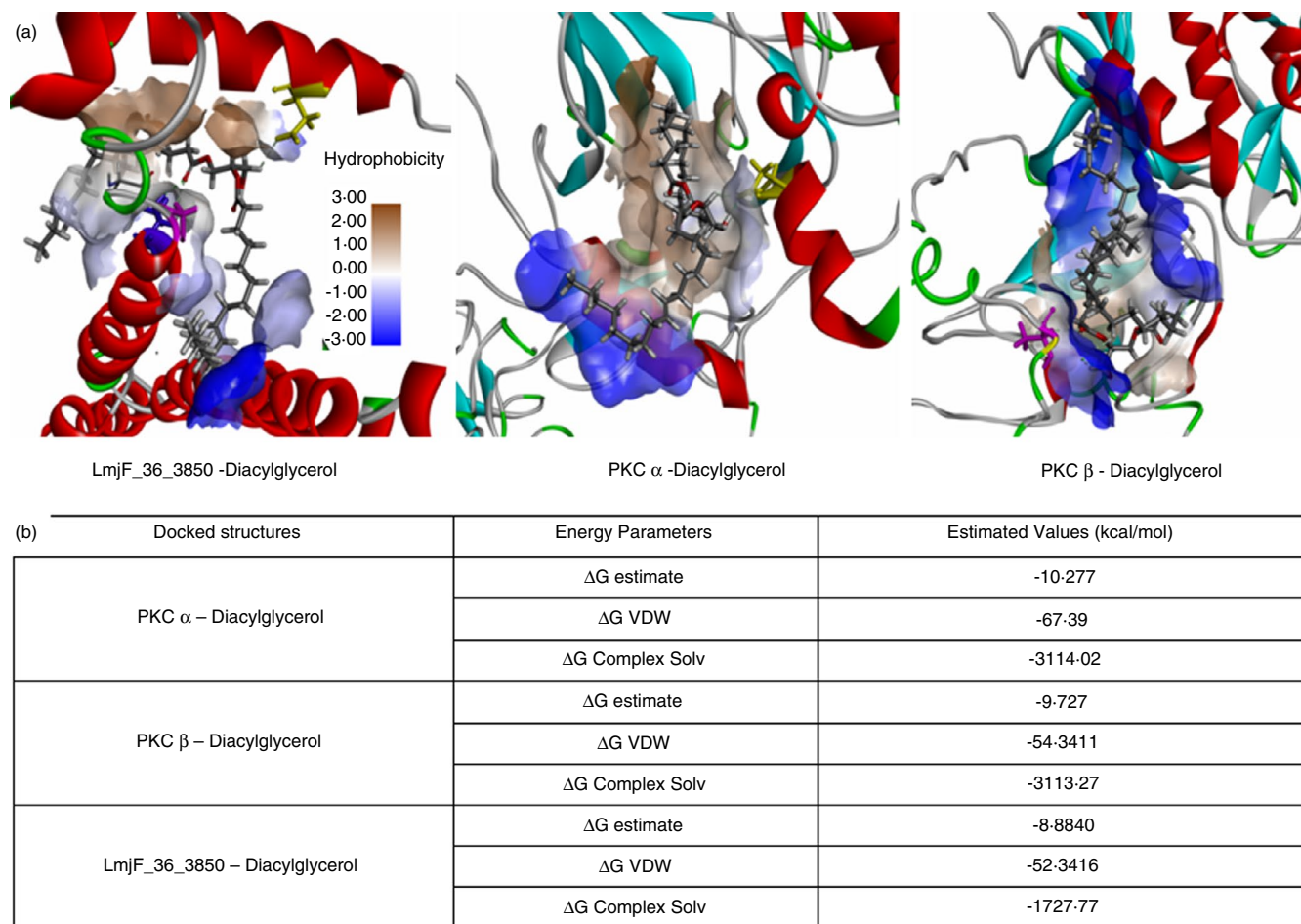


FIGURE 4 Docking models of DAG with its known and predicted ligands. (a) Docked structure of diacylglycerol with PKC α , PKC β and LmjF.36.3850. Hydrophobicity profile of DAG-interacting amino acid residues of LmjF.36.3850, PKC- α and PKC- β is shown using colour-coded hydrophobicity value bar as a reference. (b) Gibbs free energy (ΔG) values for the docked structures of PKC α , PKC β and LmjF.36.3850 with DAG

infection stage. Upregulated caveolin-1 in IM as compared to uninfected macrophage (UIM) is indicative of a successful *in vitro* infection. Immunoblotting of the cytoplasmic fraction of *L. major*-IMs revealed the presence of LmjF.36.3850, implying that this protein is secreted into the host cell cytoplasm during infection (Figure 6d). While GAPDH is used as a cytoplasmic marker, the fraction was also probed with CD40 and caveolin-1 (not detected) to confirm its purity. These structural and functional similarities between LmjF.36.3850 and Snf7 implicate LmjF.36.3850 in *L. major* virulence.

Four weeks post-priming, the levels of leishmanial antigen-specific IgG2a and IgG1, but not IgM, antibodies significantly increased in the immunized mice, as compared to the control recipients (Figure 6e). Both IgG1 and IgG2a levels had comparable rise resulting in unaltered IgG2a/IgG1 ratio (Inset, Figure 6e), an indirect measure for Th1 and Th2 subset response. DNA vaccination turned the anti-inflammatory Th17-T_{EM} and Treg-T_{EM} cells more frequent while reducing host-protective Th1-T_{EM} population (Figure 6f).

LmjF.36.3850 immunization was unable to control disease progression and parasite load, and increases the anti-inflammatory Th compartment

LmjF.36.3850-vaccinated mice showed comparable footpad swelling and LN hypertrophy, and higher, albeit insignificant, parasitic load than the control *Leishmania*-infected group (Figure 7a). These data indicate that although LmjF.36.3850 is immunogenic, it was unable to impart anti-leishmanial immune profile to vaccinated mice and curb the disease progression upon challenge infection.

qPCR analysis of cytokine transcripts in lymphocytes of *L. major*-infected BALB/c mice (control, vector primed, antigen primed) indicated that there was a significant increase in the levels of IL-4 and IL-10, but not IFN- γ , a major cytokine responsible for anti-leishmanial immunity, in the primed mice. Foxp3, a T_{reg}-associated transcription factor, and CTLA-4 (CD152), a T-cell suppressor, were found to be significantly increased in the vaccinated mice as compared to controls (Figure 7b). The levels of IL-4 and IL-10 in the primed and the infected mice were comparable, while IFN- γ

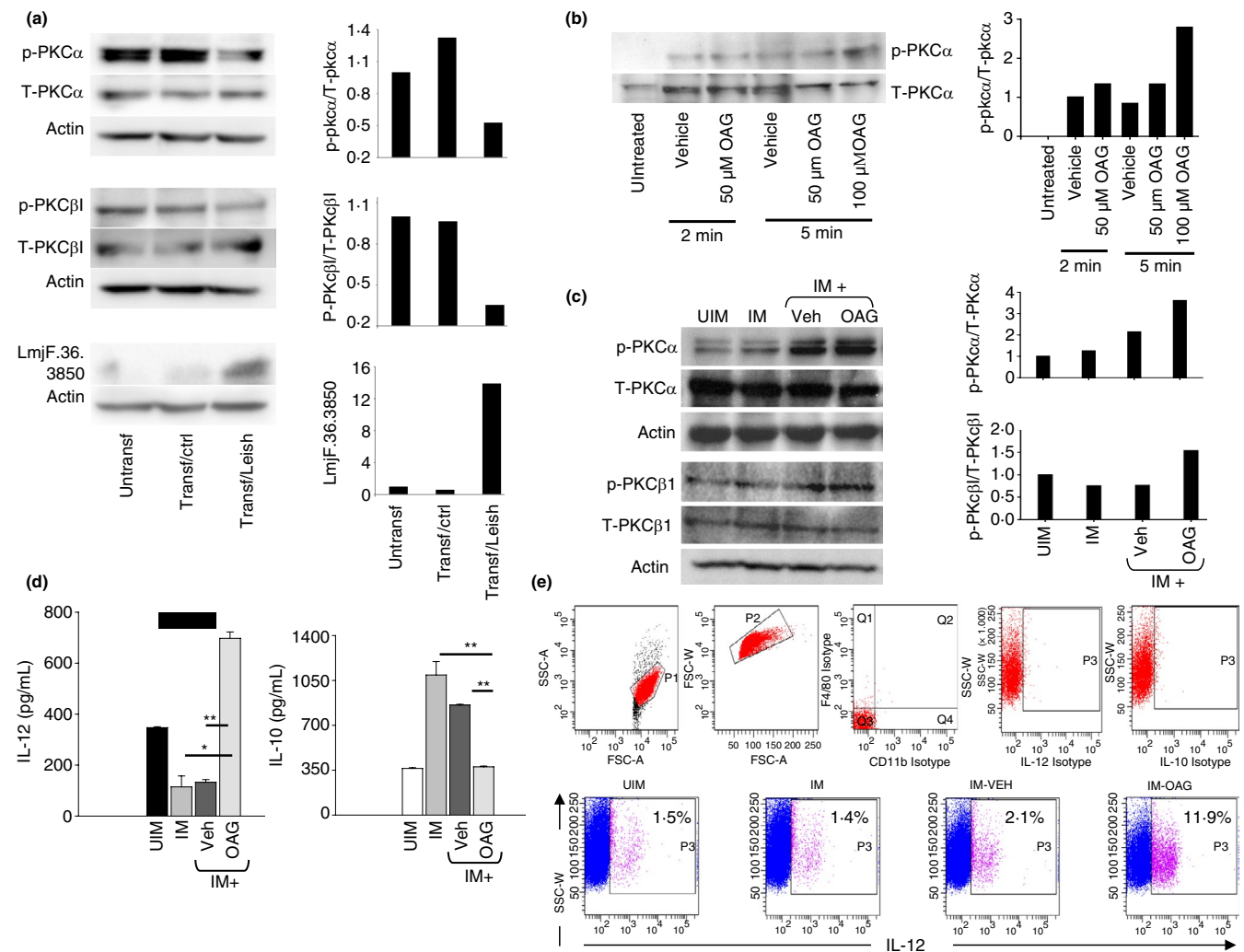


FIGURE 5 LmjF.36.3850 overexpression decreases the activation of pro-inflammatory PKCs, and OAG supplementation of *Leishmania*-infected macrophages skews the cellular response towards DAG-dependent PKC activation and pro-inflammatory cytokine pathway. (a) RAW264.7 macrophages were transfected with either control or LmjF.36.3850-pcDNA6/HisA, and phosphorylation of PKC α and PKC β was analysed by immunoblotting 48 h post-transfection. 3-h serum-starved, (b) uninfected, or (c) 36 h *L. Major*-infected RAW264.7 macrophages were supplemented with either OAG or DMSO (Veh) as indicated. Phosphorylated PKC α and PKC β (p-PKC α and p-PKC β), and total PKC α and PKC β (PKC α and PKC β) levels were determined by Western blotting, and fraction of activated PKCs was calculated by densitometry. Unstimulated (UIM) group in Fig. panel 9(a) was not included in densitometric analysis as no visual band was observed. (d) Estimation of IL-10 and IL-12 in culture supernatant of uninfected and *L. major*-infected macrophages. After 12-h infection, macrophages were supplemented with either DMSO or OAG (100 μ M) for 5 min and kept for 60 h. IL-10 and IL-12 were estimated by ELISA (OD determination at 450 nm) as described. (e) Flow cytometric analysis of IL-10-secreting macrophages upon OAG induction. After 12-h infection period, macrophages were supplemented with either DMSO or OAG (100 μ M) for 5 min, replenished with fresh media and kept for 60 h. 20 ng/ml PMA and 1 μ g/ml ionomycin were added 6 h, and BD GolgiStopTM was added 3 h prior to cell staining. Cells were stained with PECy7 anti-CD11b, APC-Cy7 anti-F4/80 and APC anti-IL-12 as described. Data are representative of two independent experiments, and error bars indicate mean \pm SEM

was significantly lower (Figure 7c). While IgG2a and IgG1 titres in LmjF.36.3850-primed mice are comparable to control vector primed mice, IgG1 production in the primed mice was lower than infected mice (Lm) (Figure 7d). As Th2 cells secrete, IL-4 induces IgG1, whereas the Th1 cell cytokine IFN- γ induces IgG2a, the IgG2a:IgG1 < 1 implied a predominant Th2 cell response in the primed mice. LmjF.36.3850 may thus suppress host-protective T cells and fail to protect mice against challenge *L. major* infection.

Priming with LmjF_36-3850 establishes the anti-inflammatory Th memory phenotype

T cells that recirculate between peripheral tissues and secondary lymphoid organs are classified as effector memory T cells (T_{EM}) and express high CD44, but low CD62L, levels, whereas memory T cells that stay in secondary lymphoid organs are central memory T cells (T_{CM}) expressing high CD44 and CD62L. Results indicate that there is an increase in the population of effector

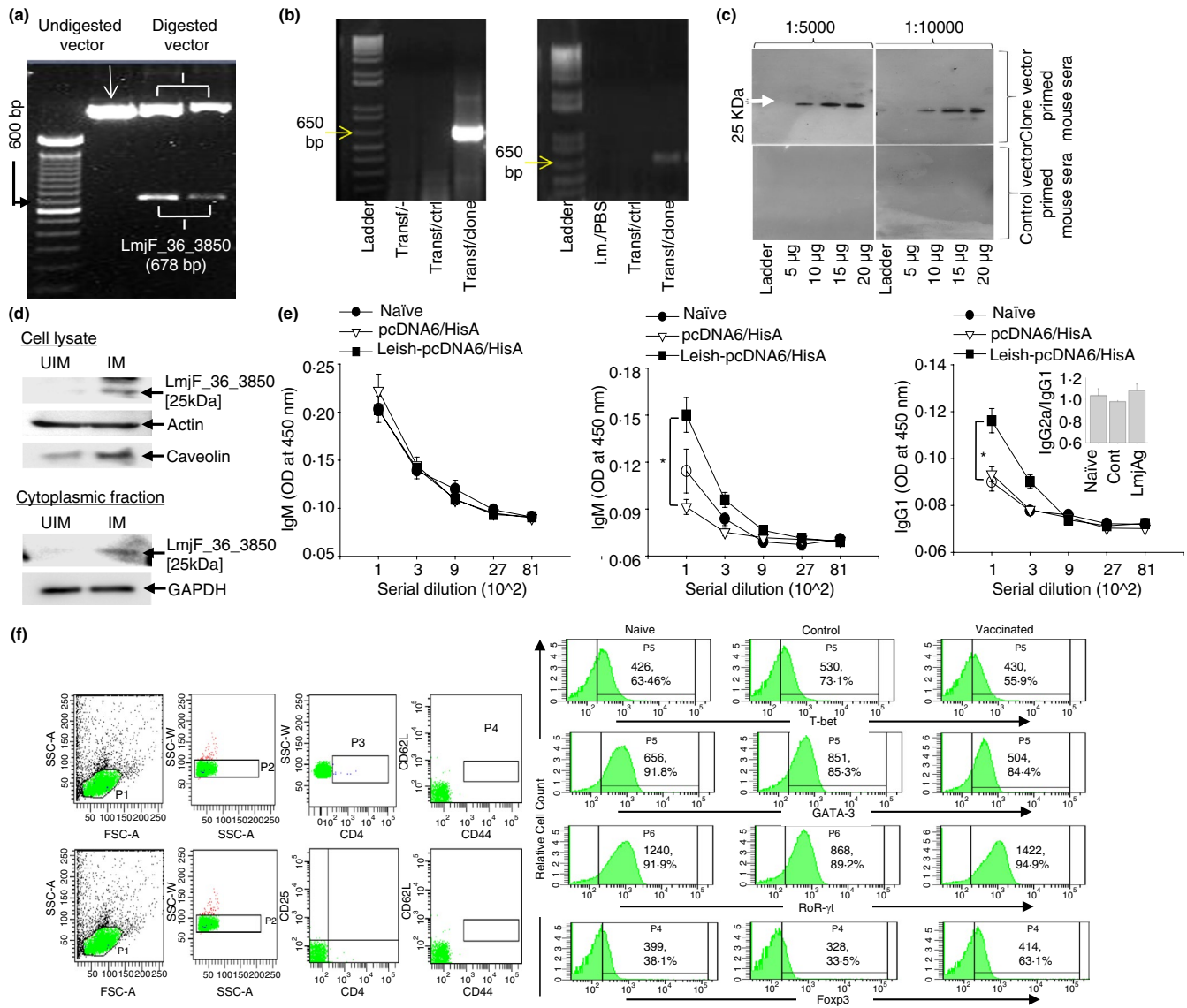


FIGURE 6 LmjF.36.3850 is present in host cell cytoplasm during intracellular infection and increases anti-inflammatory Th signature upon immunization (a) LmjF.36.3850 is cloned in pcDNA6/HisA vector (b) cDNA was prepared from the indicated groups of HEK293 T cells, left thigh muscle tissue and amplified with LmjF.36.3850 primers by RT-PCR. Data are representative of two independent experiments. (c) Whole-cell lysate of virulent *Leishmania* culture was probed with blood sera from control and immunized mice and analysed for the presence anti-LmjF.36.3850 IgG antibodies by Western blotting. (d) Whole-cell lysate (50 µg) and cytoplasmic fraction (100 µg) were probed for the presence of LmjF.36.3850 by 1:5000 dilution of DNA-vaccinated mice sera. Caveolin-1 and CD40 were used as endosomal and membrane marker to confirm the purity of cytoplasmic fraction. (e) Anti-leishmanial serum antibody isotype levels elicited by LmjF.36.3850 immunization were assessed by ELISA ($n = 5$). (f) Flow cytometric analysis of Th1-, Th2-, Th17- and Treg-T_{EM} from lymphocyte population of popliteal lymph node. Lymphocytes were stained with PB anti-CD4, APC-Cy7 anti-CD25, PECy7 anti-CD44, PerCP-Cy5.5 anti-CD62L, APC anti-T-bet/GATA-3/FOXP3 and PE anti-RORγt antibodies as described and analysed. Values inside histograms indicate the mean fluorescence intensity (MFI) of signature transcription factor (i.e. T-bet, GATA-3, RORγt and FOXP3) and percentage of respective Th-T_{EM} cells as compared to parent population. Data are representative of two independent experiments ($n = 4$)

and central memory subset of IL-10-, IL-4- and IL-17-secreting Treg, Th2 and Th17 cells, respectively, in vaccinated BALB/c mice. While the population of IFN-γ-secreting Th1 cells remains largely unchanged in T_{EM} compartment, it showed an increase in the T_{CM} compartment (Figure 8). Overall, LmjF.36.3850 priming enhances the population of anti-inflammatory memory Th cells that promote parasite persistence.

DISCUSSION

The choice of a vaccine candidate has been the trickiest in any infectious disease. In general, the virulence factors are targeted, as these are proposed to be responsible for infection and pathogenesis. Lifelong immunity conferred to cured cases of Leishmaniasis implies a probable prophylaxis

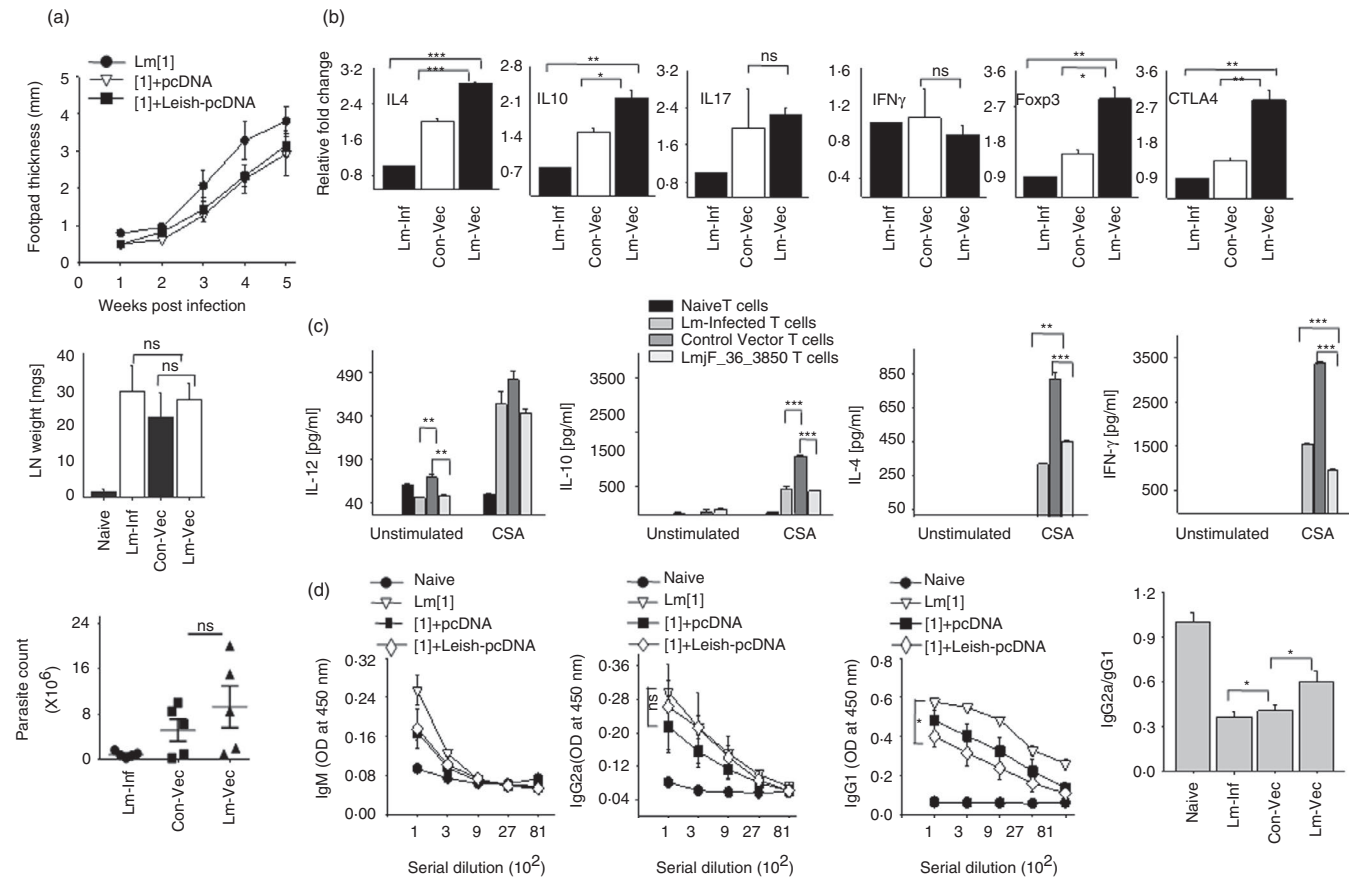


FIGURE 7 LmjF.36.3850 vaccination does not induce host-protective immune response, increases anti-inflammatory cytokine-secreting T cells and increases pro-Leishmanial IgG isotypes. (a) Footpad thickness, draining LN weight and parasite load in immunized and control mice were assessed 5 weeks after the challenge infection ($n = 5$). Data are shown as mean \pm SEM of experimental values between mice in a group. (b) qPCR analysis for the relative expression of IL-4, IL-10, IL-17, IFN- γ , FOXP3, and CTLA-4 transcripts from the lymphocytes of indicated groups of BALB/c mice, using GAPDH as housekeeping control. Each experiment was performed in duplicate, and error bars indicate SEM between duplicates. Data shown here are representative of two independent experiments. (c) IL-12, IL-10, IL-4 and IFN- γ levels in 72-h culture supernatant of unstimulated and CSA-stimulated LN cells from the indicated groups of BALB/c mice were determined by ELISA. Experiment was repeated twice, and data are shown as mean \pm SEM between duplicates. (d) Anti-leishmanial IgM, IgG2a and IgG1 titres in blood sera after 5 weeks of challenge infection were assessed by ELISA ($n = 5$). Data are shown as mean \pm SEM and are representative of two independent experiments (pcDNA: Con-Vec represents control group; and Leish-pcDNA: Lm-Vac indicates vaccinated group wherever indicated, * indicates $p \leq 0.05$, ** indicates $p \leq 0.01$, *** indicates $p \leq 0.001$)

against these factors. Selection of a vaccine candidate that elicits long-lasting host-protective immune response in the susceptible hosts appears too demanding, as *Leishmania* has many virulence factors, some of which were on clinical trial for an anti-leishmanial vaccine, but a successful vaccine is still awaited [21,42].

In this study, we attempted to identify the virulence factors of *L. major* based on the differences in the transcriptomic profile of virulent and avirulent strains. We found that the expression of LmjF.36.3850 was higher in the virulent strain of *L. major* (Table 2 and Figure 1b). Also, motif search analysis revealed its similarity with snf7 family proteins (Figure 2a), a part of ESCRT-III complex, which are essential in almost every process related to membrane budding [43] such as endosome and exosome biogenesis. More recently, importance of secretory exosomes by *Leishmania*

in the early phase of disease progression has been established [44]. LmjF.36.3850 and Snf7 primary structure alignment analyses reveal that these proteins are homologous and share similar phosphorylation sites, albeit at different positions (Figure 2b,c).

Moreover, ligand prediction via ProBiS identified DSMD, a small molecule structurally similar to DAG, as a favourable ligand for LmjF.36.3850. Further analysis revealed that Gibbs free energy (ΔG) values for LmjF.36.3850-DAG binding are similar to known DAG-binding proteins, viz. PKC α and PKC β , suggesting that LmjF.36.3850-DAG binding is thermodynamically favourable (Figures 3 and 4). This suggests that DAG-LmjF.36.3850 interaction may interfere with the activation of DAG-dependent PKC isoforms as detected during *Leishmania* infection [45]. They are the major anti-leishmanial PKCs, which lead to inflammatory

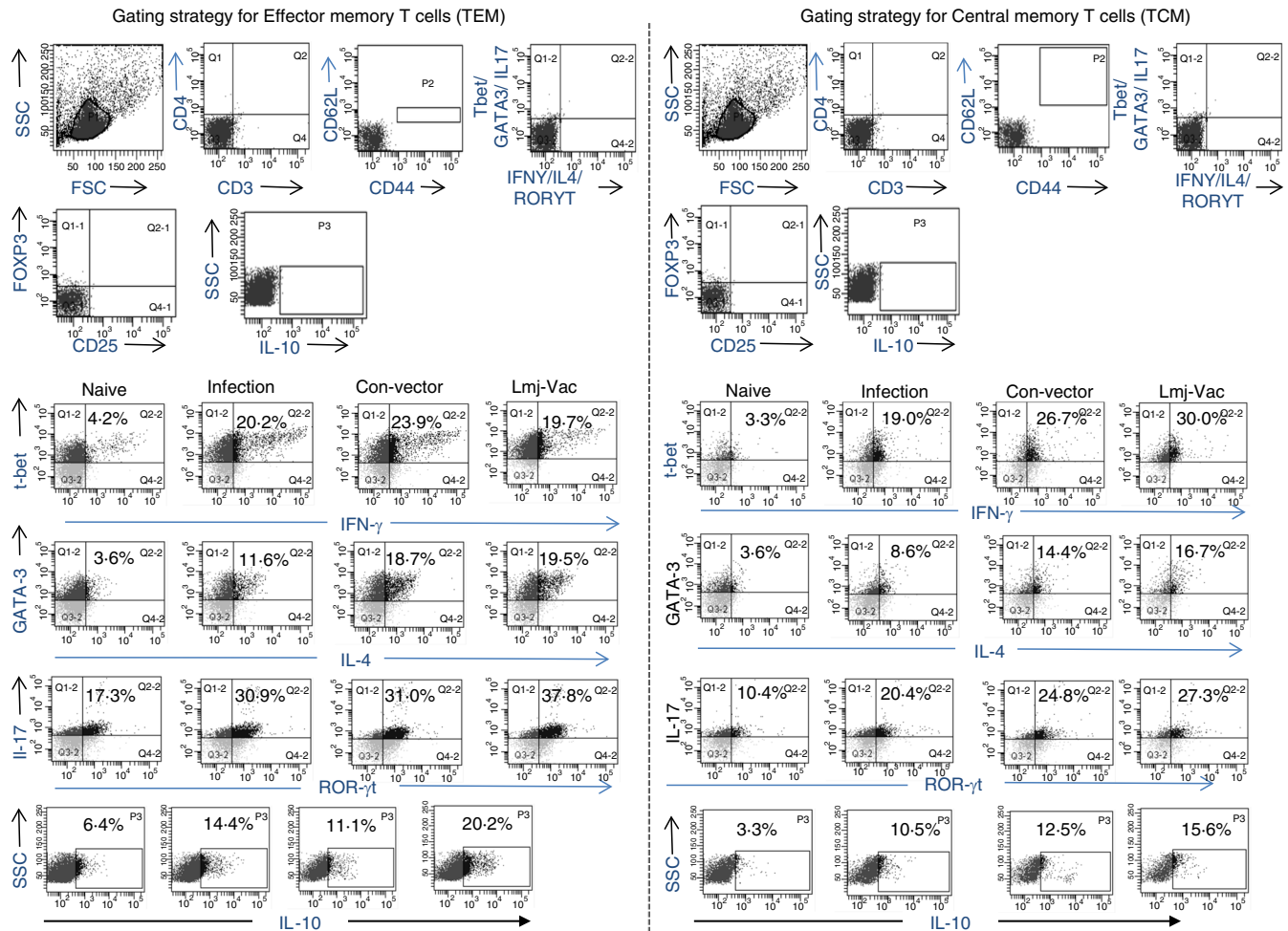


FIGURE 8 Multi-colour flow cytometry for determination of Th memory subsets. Percentage of different memory subsets (T_{EM} and T_{CM}) in different groups of BALB/c mice ($n = 5$) were assessed by seven-colour flow cytometry. LN cells from mice in a group were pooled together and stained with FITC anti-CD3, PB anti-CD4, PerCP-Cy5.5 anti-CD44, APCy7 anti-CD62L, PEcy7 anti-GITR, APC anti-Tbet, PE anti-IFN- γ , APC anti-GATA-3, PE anti-IL-4, PE anti-ROR γ t, APC anti-IL-17, APC anti-FOXP3 and PE anti-IL-10 antibody as described. CD4⁺ T cells were gated against CD44^{hi}CD62L^{hi} for determination of central memory T cells or against CD44^{hi}CD62L^{low} for determination of effector memory T cells. These were further gated for determining the percentage of cytokine-secreting Th subsets as indicated. Data shown here are representative of two independent experiments

cytokine activation and many other anti-leishmanial mechanisms inside macrophages [46]. These findings emphasize LmjF.36.3850 as a probable virulence factor for *L. major*.

Based on above observations, we assessed the immunogenicity and post-challenge protective efficacy of LmjF.36.3850 in a susceptible BALB/c mouse model. Increases in the levels of IgG1 as compared to IgG2a have been attributed to pro-leishmanial immune response and vice versa in both human CL and mouse models [47,48]. Herein, LmjF.36.3850 DNA vaccination increased IgG2a and IgG1 levels but failed to skew T-cell response towards Th1 type. Even after *L. major* challenge infection, vaccinated mice had higher levels of IgG1 antibodies as compared to IgG2a (6E, 7D). Even though the IgG2a/IgG1 ratio was higher in the vaccinated mice as compared to the controls, this was insufficient to control the progress of *L. major* infection, as the footpad lesions of the vaccinated

mice were comparable to control vector primed mice and insignificantly less than the unprimed *L. major*-infected BALB/c mice.

Expression of major immuno-regulatory cytokine IL-10, Treg-transcription factor FOXP3 and IL-4 was found to be increased in the lymphocytes of DNA-vaccinated mice as compared to controls, while the expression of IFN- γ was insignificantly decreased (Figure 7b), corroborating the previous studies that IFN- γ -associated Th1 response has been established as a major anti-leishmanial factor [49] and IL-10 promotes parasite multiplication in susceptible mice [50]. This increase in IL-10 expression may, in part, be responsible for higher parasite load observed in the vaccinated mice (Figure 7a). On the other hand, CSA restimulated cells from the LmjF.36.3850-vaccinated mice produced lower IFN- γ , while the levels of IL-4 and IL-10 remained comparable to unprimed mice. The apparent discrepancy in the recall assay

could be due to the overall cytokine profile of *Leishmania*-specific T cells, rather than LmjF.36.3850-specific T cells, rapidly proliferating after CSA stimulation following challenge infection. Enhanced CTLA-4 expression on the lymphocytes from DNA-vaccinated mice may help establish T-cell anergy and parasite persistence [51,52], suggesting pro-parasitic immuno-regulatory conditions prevailing in DNA-primed mice.

Flow cytometric analysis of Th memory subsets in study groups revealed an increase in IL-10-secreting effector and central memory Treg cells, but at the same time, there were no differences in the population of IFN- γ -secreting effector memory Th1 cells. Although an increase in central memory Th1 cells was observed, course of persistent *Leishmania* infection appears to be dictated by circulating effector memory T cells rather than central memory cells (Figure 8). These results shed light on the fact that LmjF.36.3850 priming predominantly induces naïve T cells to Treg subtype. One possible explanation is that LmjF.36.3850 may contain IL-4- and IL-10-inducing epitopes in its sequence (Table S3), although antigen-specific IL-10-producing Treg cells remain debatable [53,54].

Despite being a probable virulence factor, LmjF.36.3850 priming was unable to impart an anti-leishmanial resistance to susceptible host. Furthermore, a reduction in PKC α and PKC β 1 activation by transfection-mediated overexpression of LmjF.36.3850 (Figure 5a), and the presence of LmjF.36.3850 in *Leishmania*-IM (Figure 6d) point to the fact that LmjF.36.3850 may interact with host cellular machinery to reduce the activation of anti-leishmanial PKC isoforms – PKC α and PKC β . These two PKC isoforms were previously shown to be inhibited in *Leishmania*-IM and involved in the secretion of inflammatory cytokine, IL-12 [46]. By supplementing *L. major*-IM with PKC-activating dose of DAG analogue, viz. OAG during initial stage of infection (36 h), we observed an upregulation in the phosphorylated forms of PKC α and PKC β 1 (Figure 5b). This upregulation was linked to activation of IL-12, as OAG-supplemented IM had higher secretory levels of IL-12 and lower IL-10 (Figure 5c,d), indicating restoration of pro-inflammatory cytokine signalling. However, the restoration of PKC α and PKC β 1 phosphorylation was not seen at later stages of infection (72 h, data not shown), suggesting involvement of other evasion mechanisms at play after establishment of infection. Overall, these results point to the fact that LmjF.36.3850 may be involved in reduction in activation of anti-leishmanial PKC isoforms (α and β) by reducing DAG availability.

These results and the cytoplasmic presence of LmjF.36.3850 in IM suggest that an important parasite-derived molecule with a potential to quench DAG availability for DAG-dependent host-protective PKC isoforms may play key roles in setting up an anti-inflammatory response

and evasion of leishmanicidal functions. A new perspective associating virulence, immunogenicity and host-protective immunity may help devise a successful vaccine against *Leishmania*.

CONFLICT OF INTEREST

The authors declare that they do not have any competing financial interest or any conflicts of interest.

ORCID

Shubhranshu Zutshi  <https://orcid.org/0000-0002-5460-1683>

Bhaskar Saha  <https://orcid.org/0000-0002-5833-7912>

REFERENCES

- Awasthi A, Mathur RK, Saha B. Immune response to *Leishmania* infection. *Indian J Med Res.* 2004;119:238–58.
- Handman E, Bullen DV. Interaction of *Leishmania* with the host macrophage. *Trends Parasitol.* 2002;18:332–4.
- Gupta G, Oghumu S, Satoskar AR. Mechanisms of immune evasion in leishmaniasis. *Adv Appl Microbiol.* 2013;82:155–84.
- Scianimanico S, Desrosiers M, Dermine JF, Méresse S, Descoteaux A, Desjardins M. Impaired recruitment of the small GTPase rab7 correlates with the inhibition of phagosome maturation by *Leishmania donovani* promastigotes. *Cell Microbiol.* 1999;1:19–32.
- Vinet AF, Fukuda M, Turco SJ, Descoteaux A. The *Leishmania donovani* lipophosphoglycan excludes the vesicular proton-ATPase from phagosomes by impairing the recruitment of synaptotagmin V. *PLoS Pathog.* 2009;5:e1000628.
- Barr SD, Gedamu L. Role of peroxidoxins in *Leishmania chagasi* survival. Evidence of an enzymatic defense against nitrosative stress. *J Biol Chem.* 2003;278:10816–23.
- Jacques I, Andrews NW, Huynh C. Functional characterization of LIT1, the *Leishmania amazonensis* ferrous iron transporter. *Mol Biochem Parasitol.* 2010;170:28–36.
- de Mendonça SC, Cysne-Finkelstein L, Matos DC. Kinetoplastid membrane protein-11 as a Vaccine Candidate and a virulence factor in *Leishmania*. *Front Immunol.* 2015;6:524.
- Singh B, Sundar S. Leishmaniasis: vaccine candidates and perspectives. *Vaccine* 2012;30:3834–42.
- Nagill R, Kaur S. Vaccine candidates for leishmaniasis: a review. *Int Immunopharmacol.* 2011;11:1464–88.
- Pinheiro RO, Pinto EF, de Matos Guedes HL, Filho OA, de Mattos KA, Saraiva EM, et al. Protection against cutaneous leishmaniasis by intranasal vaccination with lipophosphoglycan. *Vaccine* 2007;25:2716–22.
- Martínez Salazar MB, Delgado Domínguez J, Silva Estrada J, González Bonilla C, Becker I. Vaccination with *Leishmania mexicana* LPG induces PD-1 in CD8⁺ and PD-L2 in macrophages thereby suppressing the immune response: a model to assess vaccine efficacy. *Vaccine* 2014;32:1259–65.
- Bhaumik S, Basu R, Sen S, Naskar K, Roy S. KMP-11 DNA immunization significantly protects against *L. donovani* infection but requires exogenous IL-12 as an adjuvant for comparable protection against *L. major*. *Vaccine* 2009;27:1306–16.

14. Khamesipour A, Rafati S, Davoudi N, Maboudi F, Modabber F. Leishmaniasis vaccine candidates for development: a global overview. *Indian J Med Res.* 2006;123:423–38.
15. Handman E. Leishmaniasis: current status of vaccine development. *Clin Microbiol Rev.* 2001;14:229–43.
16. Noazin S, Modabber F, Khamesipour A, Smith PG, Moulton LH, Nasser K, et al. First generation leishmaniasis vaccines: a review of field efficacy trials. *Vaccine* 2008;26:6759–67.
17. Chhajer R, Ali N. Genetically modified organisms and visceral leishmaniasis. *Front Immunol.* 2014;5:213.
18. Coler RN, Reed SG. Second-generation vaccines against leishmaniasis. *Trends Parasitol.* 2005;21:244–9.
19. Selvapandiyani A, Dey R, Gannavaram S, Lakhal-Naouar I, Duncan R, Salotra P, et al. Immunity to visceral leishmaniasis using genetically defined live-attenuated parasites. *J Trop Med.* 2012;2012:631460.
20. De Brito RCF, Cardoso JMO, Reis LES, Vieira JF, Mathias FAS, Roatt BM, et al. Peptide Vaccines for Leishmaniasis. *Front Immunol.* 2018;9:1043.
21. Gillespie PM, Beaumier CM, Strych U, Hayward T, Hotez PJ, Bottazzi ME. Status of vaccine research and development of vaccines for leishmaniasis. *Vaccine* 2016;34:2992–5.
22. Iborra S, Solana JC, Requena JM, Soto M. Vaccine candidates against *Leishmania* under current research. *Expert Rev Vaccines.* 2018;17:323–34.
23. Jha MK, Sarode AY, Bodhale N, Mukherjee D, Pandey SP, Srivastava N, et al. Development and characterization of an avirulent *Leishmania major* strain. *J Immunol.* 2020;204:2734–53.
24. Mathur RK, Awasthi A, Wadhwa P, Ramanamurthy B, Saha B. Reciprocal CD40 signals through p38MAPK and ERK-1/2 induce counteracting immune responses. *Nat Med.* 2004;10:540–4.
25. Awasthi A, Mathur R, Khan A, Joshi BN, Jain N, Sawant S, et al. CD40 signaling is impaired in *L. major*-infected macrophages and is rescued by a p38MAPK activator establishing a host-protective memory T cell response. *J Exp Med.* 2003;197:1037–43.
26. Chandel HS, Pandey SP, Shukla D, Lalsare K, Selvaraj SK, Jha MK, et al. Toll-like receptors and CD40 modulate each other's expression affecting *Leishmania major* infection. *Clin Exp Immunol.* 2014;176:283–90.
27. Marchler-Bauer A, Derbyshire MK, Gonzales NR, Lu S, Chitsaz F, Geer LY, et al. CDD: NCBI's conserved domain database. *Nucleic Acids Res.* 2015;43:D222–6.
28. Finn RD, Coghill P, Eberhardt RY, Eddy SR, Mistry J, Mitchell AL, et al. The Pfam protein families database: towards a more sustainable future. *Nucleic Acids Res.* 2016;44:D279–85.
29. Finn RD, Attwood TK, Babbitt PC, Bateman A, Bork P, Bridge AJ, et al. InterPro in 2017-beyond protein family and domain annotations. *Nucleic Acids Res.* 2017;45:D190–9.
30. Sigrist CJA, De Castro E, Cerutti L, Cuche BA, Hulo N, Bridge A, et al. New and continuing developments at PROSITE. *Nucleic Acids Res.* 2013;41:344–7.
31. Sievers F, Wilm A, Dineen D, Gibson TJ, Karplus K, Li W, et al. Fast, scalable generation of high-quality protein multiple sequence alignments using Clustal Omega. *Mol Syst Biol.* 2011;7:539.
32. Roy A, Kucukural A, Zhang Y. I-TASSER: a unified platform for automated protein structure and function prediction. *Nat Protoc.* 2010;5:725–38.
33. Konc J, Miller BT, Štular T, Lešnik S, Woodcock HL, Brooks BR, et al. ProBiS-CHARMMing: web interface for prediction and optimization of ligands in protein binding sites. *J Chem Inf Model.* 2015;55:2308–14.
34. Sadler JB, Lamb CA, Gould GW, Bryant NJ. Complete membrane fractionation of 3T3-L1 adipocytes. *Cold Spring Harb Protoc.* 2016;2016. pdb.prot083691.
35. Kumari S, Singh S, Saha B, Paliwal PK. *Leishmania major* MAP kinase 10 is protective against experimental *L. major* infection. *Vaccine* 2011;29:8783–7.
36. Rub A, Dey R, Jadhav M, Kamat R, Chakkaramakkil S, Majumdar S, et al. Cholesterol depletion associated with *Leishmania major* infection alters macrophage CD40 signalosome composition and effector function. *Nat Immunol.* 2009;10:273–80.
37. Kallas EG, Gibbons DC, Soucier H, Fitzgerald T, Treanor JJ, Evans TG. Detection of intracellular antigen-specific cytokines in human T cell populations. *J Infect Dis.* 1999;179:1124–31.
38. Nucleotide [Internet]. Bethesda, MD: National Library of Medicine (US), National Center for Biotechnology Information; 2005. Accession No. XM_001686916.1, *Leishmania major* strain Friedlin conserved hypothetical protein partial mRNA; [cited 2018 05 29]. Available from: https://www.ncbi.nlm.nih.gov/nucleotide/NM_001349333.1.
39. Tang S, Henne WM, Borbat PP, Buchkovich NJ, Freed JH. Structural basis for activation, assembly and membrane binding of ESCRT-III Snf7 filaments. *Elife.* 2015;15:e12548.
40. Godinho RM, Crestani J, Kmetzsch L, Araujo Gde S, Frases S, Staats CC. The vacuolar-sorting protein Snf7 is required for export of virulence determinants in members of the *Cryptococcus neoformans* complex. *Sci Rep.* 2014;4:6198.
41. Eliyahu E, Shalgi R. A role for protein kinase C during rat egg activation. *Biol Reprod.* 2002;67:189–95.
42. Rezvan H, Moafi M. An overview on *Leishmania* vaccines: a narrative review article. *Vet Res Forum Winter.* 2015;6:1–7.
43. Alonso Y, Adell M, Migliano SM, Teis D. ESCRT-III and Vps4: a dynamic multipurpose tool for membrane budding and scission. *FEBS J.* 2016;283:3288–302.
44. Atayde VD, Aslan H, Townsend S, Hassani K, Kamhawi S, Olivier M. Exosome secretion by the parasitic protozoan *Leishmania* within the Sand Fly Midgut. *Cell Rep.* 2015; 13:957–67.
45. Sudan R, Srivastava N, Pandey SP, Majumdar S, Saha B. Reciprocal regulation of protein kinase C isoforms results in differential cellular responsiveness. *J Immunol.* 2012;188:2328–37.
46. Shadab M, Ali N. Evasion of host defence by *Leishmania donovani*: subversion of signaling pathways. *Mol Biol Int.* 2011;2011:343961.
47. Ozbilge HN, Gurel Aksoy MS, Yazar S. IgG and IgG subclass antibodies in patients with active cutaneous leishmaniasis. *J Med Microbiol.* 2006;55:1329–31.
48. Rostamian MS, Sohrabi S, Kavosifard H, Niknam HM. Lower levels of IgG1 in comparison with IgG2a are associated with protective immunity against *Leishmania tropica* infection in BALB/c mice. *J Microbiol Immunol Infect.* 2017;50:160–6.
49. Kima PE, Soong L. Interferon gamma in leishmaniasis. *Front Immunol.* 2013;4:156.
50. Noben-Trauth N, Lira R, Nagase H, Paul WE, Sacks DL. The relative contribution of IL-4 receptor signaling and IL-10 to susceptibility to *Leishmania major*. *J Immunol.* 2003;170:5152–8.
51. Zubairi S, Sanos SL, Hill S, Kaye PM. Immunotherapy with OX40L-Fc or anti-CTLA-4 enhances local tissue responses and killing of *Leishmania donovani*. *Eur J Immunol.* 2004;34:1433–40.
52. Saha B, Chattopadhyay S, Germond R, Harlan DM, Perrin PJ. CTLA4 (CD152) modulates the Th subset response and alters

- the course of experimental *Leishmania major* infection. Eur J Immunol. 1998;28:4213–20.
53. Watt WC, Cecil DL, Disis ML. Selection of epitopes from self-antigens for eliciting Th2 or Th1 activity in the treatment of auto-immune disease or cancer. Semin Immunopathol. 2017;39:245–53.
54. Liew FY, Millott SM, Schmidt JA. A repetitive peptide of *Leishmania* can activate T helper type 2 cells and enhance disease progression. J Exp Med. 1990;172:1359–65.

SUPPORTING INFORMATION

Additional supporting information may be found online in the Supporting Information section.

How to cite this article: Zutshi S, Sarode AY, Ghosh SK, et al. LmjF.36.3850, a novel hypothetical *Leishmania major* protein, contributes to the infection. *Immunology*. 2021;163:460–477. <https://doi.org/10.1111/imm.13331>